SCIENCE CHINA
Chemistry

•ARTICLES•
SPECIAL ISSUE: Celebrating the 60th Anniversary of the University of Science and Technology of China

September 2018 Vol.61 No.9: 1167–1174
https://doi.org/10.1007/s11426-018-9321-0

Effective conversion of cellobiose and glucose to sorbitol using non-noble bimetallic NiCo/HZSM-5 catalyst

Bakht Zada[†], Long Yan[†] & Yao Fu[*]

Hefei National Laboratory for Physical Science at the Microscale, Collaborative Innovation Center of Chemistry for Energy Materials (iChEM), CAS Key Laboratory of Urban Pollutant Conversion, Anhui Province Key Laboratory for Biomass Clean Energy and Department of Chemistry, University of Science and Technology of China, Hefei 230026, China

Received March 21, 2018; accepted June 28, 2018; published online August 3, 2018

The tandem hydrolysis and hydrogenation of saccharides into sorbitol is an especially attractive reaction in the conversion of biomass. Here, an economical and efficient bimetallic catalyst for the transformation of glucose and cellobiose into sorbitol is reported. Non-precious metal based catalysts such as NiCo, Ni, and Co, were prepared via modified impregnation method, and NiCo/HZSM-5 showed superior performance for the synthesis of sorbitol (86.9% from cellobiose, 98.6% from *D*-glucose). Various characterizations, such as Brunner-Emmet-Teler (BET), X-ray diffraction (XRD), transmission electron microscopy (TEM) and X-ray photoelectron spectroscopy (XPS), confirmed that NiCo alloy formed and highly dispersed in NiCo/HZSM-5 catalyst. The high performance of fabricated catalyst would be attributed to the formation of nickel-cobalt alloy over HZSM-5 zeolite surface. High temperature and H_2 pressure were favorable for the tandem hydrolysis and hydrogenation reaction. Besides, the reaction pathway was also proposed based on the kinetics study. Cellobitol was detected as the intermediate in the reaction mixture. Furthermore, in the catalytic stability study, it was found that active metal species of NiCo/HZSM-5 were stable. The deactivation of catalyst would be due to the covering of acidic sites over NiCo/HZSM-5.

biomass, sorbitol, glucose, cellobiose, bimetallic catalyst

Citation: Zada B, Yan L, Fu Y. Effective conversion of cellobiose and glucose to sorbitol using non-noble bimetallic NiCo/HZSM-5 catalyst. *Sci China Chem*, 2018, 61: 1167–1174, https://doi.org/10.1007/s11426-018-9321-0

1 Introduction

Global resources crisis is a serious problem for today's human society. Replacing the traditional fossil resources with renewable biomass is a commonly acknowledged guideline for the future liquid fuel productions. What's more, the utilization of renewable resources would have a positive impact on the environment [1]. Lignocellulose, as one of the most abundant biomass, has been converted to chemicals and liquid fuels by various techniques, such as fast pyrolysis, thermal gasification, enzymatic fermentation and chemical catalysis [2–5]. Sugar alcohols are type of representative products, which would be synthesized from lignocelluloses via tandem hydrolysis and hydrogenation [6]. Sorbitol, the main product of cellulose tandem hydrolysis and hydrogenation, is one of the most important industrial chemicals, which has been listed as one of the top 12 biomass-derived platform chemicals by U.S department of energy [7]. It is widely used for many applications such as food additive, cosmetic industries, medicines and fuel synthesis [7,8]. Currently, the production of sorbitol is mostly carried out by directly hydrogenation of glucose, and the substrates is mainly obtained by hydrolysis of various starches such as

†These authors contributed equally to this work.
*Corresponding author (email: fuyao@ustc.edu.cn)

rice, potato and corn. [9]. However, it would be more appropriate to use non-edible precursors such as cellulose and di-saccharides for the synthesis of sorbitol [9,10]. In this regard, the non-edible cellobiose, which could produce with high yield from cellulose [11,12], becomes an ideal substrate for the synthesis of sorbitol.

Since cellobiose molecule is comprised of two glucose monomers via 1,4-β-glycoside bond, the synthesis of sorbitol from cellobiose has to go through the tandem hydrolysis and hydrogenation processes. Hence, bifunctional catalysts and catalytic systems were continuously developed for this conversion [12–16]. In 2006, Liu *et al*. [12] found that Ru nanoparticles dispersed in an acidic aqueous medium (pH 2.0) could efficiently catalyzed converting the cellobiose into sorbitol. Noteworthily, the authors found that acidic reaction environment was a necessary condition. New carbon-based materials, such as carbon-nanotubes (CNTs) and modified activated carbon have been widely applied in the catalyst fabrications, since their high hydrothermal stability and surface paintability [13]. Wang *et al*. [4] reported the acidic groups modified CNTs supported Ru nanoparticles catalyst for the conversion of cellobiose. 87% yield of sorbitol was obtained at 150 °C and 2 MPa H_2 within 30 min. Cellobitol was confirmed as the key intermediate in this transformation. Heeres *et al*. [11] developed mesoporous carbon supported Ru catalyst (Ru/CMK-3) for the conversion of cellobiose. 91.1% yield of sorbitol was given at 180 °C and 5 MPa H_2 over Ru/CMK-3 catalyst in aqueous phase. The excellent catalytic activity was due to abundant strong acid sites in the Ru/CMK-3 catalyst. Recently, Lopez-Sanchez *et al*. [14] synthesized a bi-functional Ru catalyst with strong acidic resin A-15 (Amberlyst-15) for the same conversion. 81% yield of sorbitol was formed over 3% RuNps/A15 within 5 h. Pereira *et al*. [15] discovered that introducing Ni into the Ru based catalysts would obviously improve the catalytic activity. Similarly, Alonso *et al*. [16] found that the catalytic activity of Ni/MCM-48 was remarkably improved with introducing trace Ru metal. However, non-noble metal based catalysts were barely reported for the conversion of cellobiose. Considering the high cost of noble metal based catalysts, non-noble metal based catalysts are more attractive for the large-scale application.

In this work, various HZSM-5 supported non-precious metal based catalysts (i.e. NiCo/HZSM-5, Ni/HZSM-5, and Co/HZSM-5) were prepared through step impregnation method and tested for the synthesis of sorbitol. The reaction temperature and H_2 pressure both showed an obvious impact on the catalytic performance and the highest catalytic activity was observed over the NiCo/HZSM-5 catalyst. The formation of NiCo alloy was confirmed by X-ray diffraction (XRD), X-ray photoelectron spectroscopy (XPS), energy dispersive X-ray spectroscopy (EDX) and transmission electron microscopy (TEM) characterizations. Compared with the mono-metallic catalysts, the superior performance was possibly due to the alloy species. In the kinetic studies, cellobitol was detected as the key intermediate. Furthermore, NiCo/HZSM-5 showed a well stability for the catalyzed conversion.

2 Experimental

2.1 Materials

Cellobiose, glucose, and sorbitol were purchased from J&K Scientific Ltd. (China). $Ni(NO_3)_2{\cdot}6H_2O$ and $Co(NO_3)_2{\cdot}6H_2O$ were purchased from Sinopharm Chemical Reagent Co. Ltd. (China). HZSM-5 zeolite (Si/Al=25), HY, and MOR were purchased from Nankai University Catalyst Co., Ltd. (China). Cellobitol was prepared by using previously reported method [17] and analyzed by using liquid chromatography mass spectrometry (LC-MS) and high performance liquid chromatography (HPLC).

2.2 Catalyst preparation

HZSM-5 supported catalysts were prepared via a step impregnation method. 5.0 g HZSM-5 zeolite was impregnated with 1.45 g $Co(NO_3)_2$. The mixture was stirred for 12 h at 25 °C and dried at 105 °C over night. The dried sample were re-dissolved with 2.91 g $Ni(NO_3)_2$ in water and stirred for another 12 h under room temperature. After that, the water was evaporated from the solution and the solids were dried at 105 °C. The catalysts were calcined at 400 °C in N_2 and reduced at 500 °C in the presence of N_2/H_2 as reported in our previous work [18]. The loadings of Ni and Co were respectively 10% and 5%. Other supported catalysts were also fabricated in the same way. Experimental details of characterization are described in the Supporting Information online.

2.3 Conversion of glucose and cellobiose

The catalyzed conversions of glucose and cellobiose were carried out in 25 mL Parr reactor equipped with a manganic stirrer. In a typical experiment, a solution containing substrate (1 M glucose or 0.5 M cellobiose), 100 mg catalyst and 12 mL deionised water was injected into the reactor. The reactor was flushed five times with H_2 to remove air and maintained at specifies hydrogen pressure (1–6 MPa). The sealed reactor was heated to desired temperature with a heating rate of 10 °C/min at 1000 r/min. The reaction temperature was maintained at a certain value, i.e. in a range of 100 to 200 °C for 1–6 h. After the reaction, the reactor was cooled to room temperature and the product mixture was collected and analyzed by HPLC.

3 Results and discussion

3.1 Catalyst characterizations

The physicochemical properties of catalysts were shown in Table 1. After the introduction of metal, the surface area of HZSM-5 was obviously decreased. With Ni loading, the Brunauer-Emmett-Teller surface area (S_{BET}) of HZSM-5 decreased from 208.17 to 55.24 m^2/g. Interestingly, the S_{BET} of Co/HZSM-5 was 16.57 m^2/g that reduced more obviously than the parameter of Ni/HZSM-5. Similarly, the surface area of bimetallic NiCo/HZSM-5 catalyst further decreased to 13.64 m^2/g. The pore volumes and sizes of HZSM-5 and supported catalysts changed in the similar rule. With the introduction of metal, the pore parameters of HZSM-5 reduced gradually. Similar results were also reported in previous works [19,20].

To confirm the formation of Ni and Co metal nanoparticles, all the materials were characterized through XRD, as shown in Figure 1. All the characterized peaks of HZSM-5 would be found in the XRD results of catalysts. Meanwhile, the characterized peaks of Ni metal were found at 2θ=44.6°, 51.9° and 75.4° in the results of Ni/HZSM-5 catalysts, reflecting the formation of Ni nanoparticles. However, no characteristic peaks of Co species were observed in Co/HZSM-5 that would possibly be due to the relatively low loading of Co and its high dispersion. Noteworthily, slight shifts of metallic characterized peaks (indicated by dotted lines) were detected in the XRD patterns of NiCo/HZSM-5 and reused NiCo/HZSM-5 catalysts, that may reflect the formation of NiCo alloy [21]. In order to confirm this hypothesis, all catalysts were analyzed through XPS characterizations.

As shown in Figure 2(a), XPS spectra for Ni2p of Ni/HZSM-5 catalyst at 852.8±0.1 and 869.9±0.1 eV are ascribed to metallic nickel (Ni^0) in the $Ni^0 2p_{3/2}$ and $Ni^0 2p_{1/2}$ level, respectively [22]. While the binding energies for $Ni^0 2p_{3/2}$ and $Ni^0$2p1/2 level of NiCo/HZSM-5 were observed at 853.0±0.1 and 870.3±0.1 eV respectively. The peaks at 856.0±0.1 and 873.6±0.1 eV are assigned to oxidized nickel (Ni^{2+}) in the $Ni^{2+}2p_{3/2}$/$Ni^{2+}2p_{1/2}$ level, along with two satellite peaks around 861.1±0.1 and 880.8±0.2 eV, respectively. The oxidized Ni might be formed by the contact with air before measurement. The binding energies for NiCo/HZSM-5 at 778.14±0.1 and 793.4±0.1 eV are ascribed to metallic cobalt (Co^0) in the $Co^0 2p_{3/2}$/Co^0 $2p_{1/2}$ level, respectively. The oxidized cobalt (Co^{2+}) in the $Co^{2+}2p_{3/2}$/$Co^{2+}2p_{1/2}$ level is also observed corresponding to the binding energy of 781.4±0.1 and 797.1±0.1 eV [22]. Since the samples were exposed in air, the contents of oxidized phases (Ni^{2+}, Co^{2+} species) might be increased. However, for Co/HZSM-5 only oxidized $Co^0 2p_{3/2}$, $Co^0 2p_{1/2}$ and satellite peaks were observed. The binding energy results reflected that the Ni shifted from low oxidation to high oxidation state, and the Co shifted to low

Table 1 Physio-chemical properties of catalysts

Catalyst	S_{BET} (m^2/g)	V_p (cm^3/g) [a]	D_p (nm) [b]
HZSM-5	208.17	0.097	1.95
Ni/HZSM-5	55.24	0.061	1.43
Co/HZSM-5	16.57	0.018	1.93
NiCo/HZSM-5	13.64	0.015	1.42

a) V_p is single point adsorption total pore volume of pores; b) D_p is adsorption average pore width.

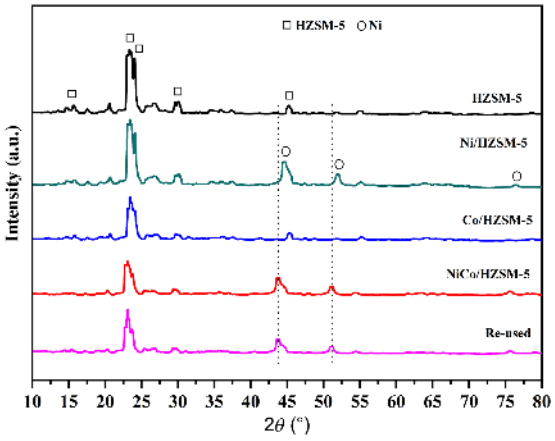

Figure 1 XRD patterns of HZSM-5, Ni/HZSM-5, Co/HZSM-5, NiCo/HZSM-5 and used NiCo/HZSM-5 catalysts (color online).

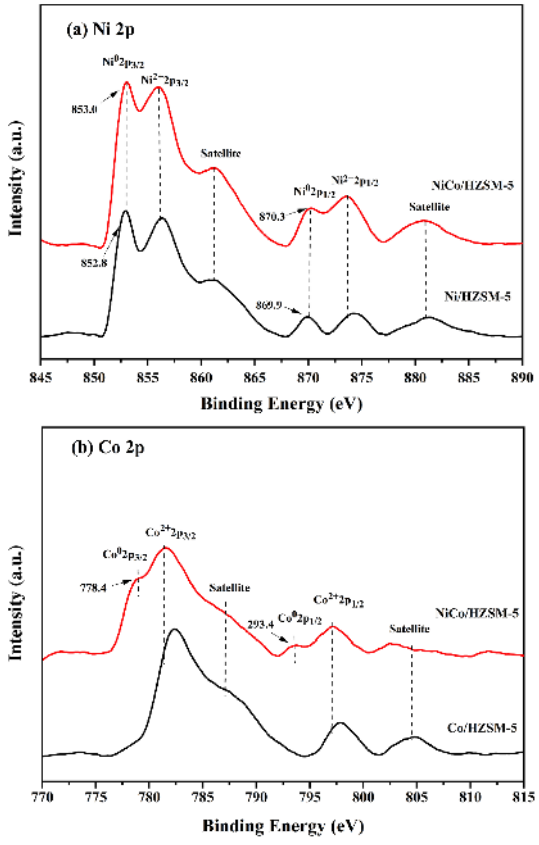

Figure 2 XPS spectra of (a) Ni2p and (b) Co2p of Ni/HZSM-5, Co/HZSM-5 and NiCo/HZSM-5 catalysts (color online).

oxidation state, indicating the partial electronic transfer between Ni and Co in NiCo alloy catalyst. The surface valance bond spectra also support the respective electronic interaction between Ni and Co species (Figure S3, Supporting Information online) [23,24]. The electron transformation in NiCo/HZSM-5 catalyst would protect metallic sites from oxidation during the reaction, as reported in previous references [25,26]. Meanwhile, the interaction between Ni and Co on the surface of catalyst confirmed the formation of Ni–Co alloy during reduction operation [22,23,27,28].

To find the morphologies of catalysts, TEM characterizations were conducted. As shown in Figure 3(a), highly dispersed Co nanoparticles were observed in the TEM image of Co/HZSM-5. The EDS results confirmed the existing of Co species. The above phenomena reflected that, the cobalt species were highly dispersed over the surface of Co/HZSM-5 catalyst. Obvious Ni nanoparticles were observed in the TEM images of Ni/HZM-5 and NiCo/HZM-5 catalysts. The average sizes of Ni nanoparticles over Ni/HZM-5 and NiCo/HZM-5 catalysts were 5.0 and 4.8 nm respectively. Furthermore, as shown in Figure 3(g), the EDX mapping results for Ni and Co elemental distribution of bimetallic NiCo/HZSM-5 catalyst showed approximately homogeneous Ni and Co species in metallic nanoparticles of catalyst, confirming the formation of NiCo alloy [21].

3.2 Conversion of glucose and cellobiose into sorbitol

Conversion of glucose into sorbitol via catalyzed hydrogenation was employed as model reaction to study the catalytic activities of HZSM-5 supported catalysts. The Ni/HZSM-5 and Co/HZSM-5 catalysts gave 67% and 22% yields for sorbitol with 80% and 27% conversions of glucose respectively, as shown in entry 1 and 2 of Table 2. Fortunately, the yield of sorbitol was remarkably elevated to 98% over the NiCo/HZSM-5 catalyst (entry 3). To compare the results, the physical mixture of Ni/HZSM-5 and Co/HZSM-5 was also tested in this catalytic system. As ex-

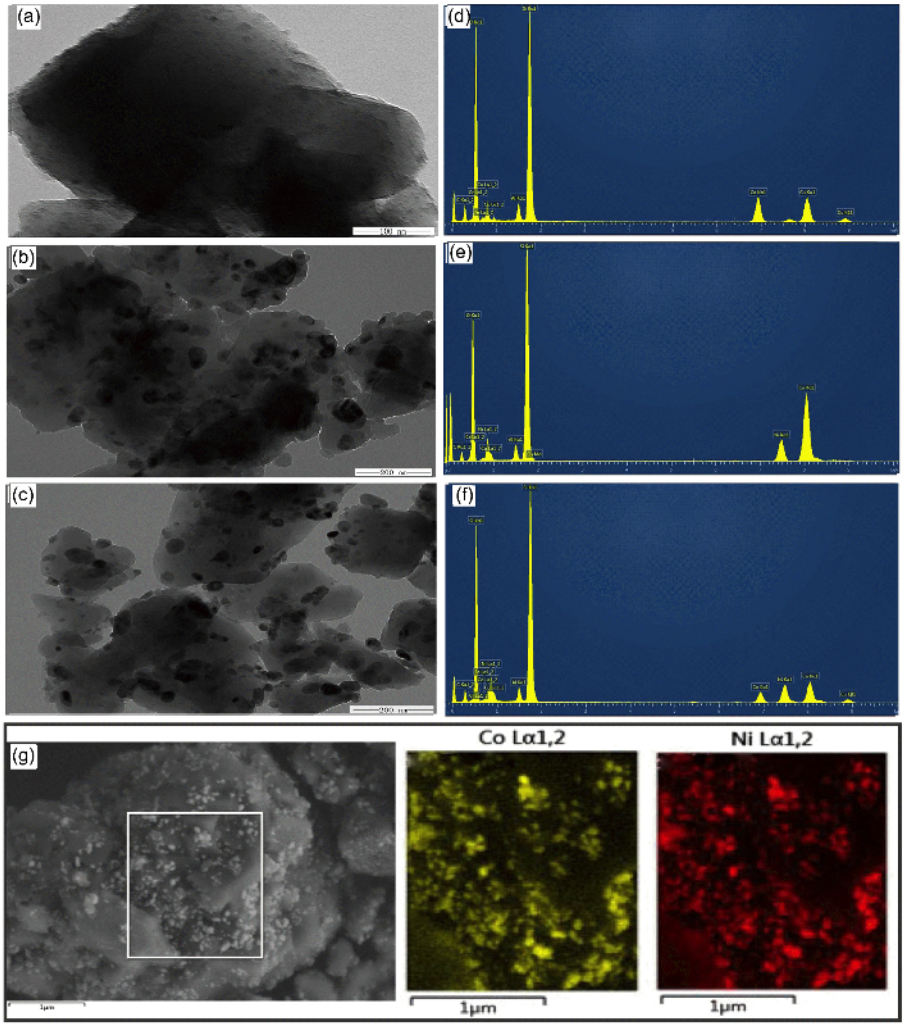

Figure 3 TEM images of (a) Co/HZSM-5, (b) Ni/HZSM-5, (c) NiCo/HZSM-5, and EDX patterns of (d) Co/HZSM-5, (e) Ni/HZSM-5, (f) NiCo/HZSM-5 catalysts. (g) Scanning electron microscope (SEM)-EDX mapping image of the NiCo/HZSM-5 (color online).

Table 2 Catalysts screening for the conversion of glucose and cellobiose into sorbitol [a)]

Entry	Catalyst	Substrate	Conversion (%)	Yield (%)
1	Ni/HZSM-5	Glucose	80	67
2	Co/HZSM-5	Glucose	27	22
3	NiCo/HZSM-5	Glucose	100	98
4	Ni/HZSM-5+ Co/HZSM-5	Glucose	90	86
5	NiCo/HY	Glucose	94	89
6	NiCo/MOR	Glucose	86	81
7	NiCo/HZSM-5	Cellobiose	100	86
8	Ni/HZSM-5	Cellobiose	100	72
9	Co/HZSM-5	Cellobiose	17	8
10	NiCo/AC	Cellobiose	80	32
11	NiCo/HY	Cellobiose	92	73
12	NiCo/MOR	Cellobiose	84	42
13	NiCo/HZSM-5	Sorbitol	–	92

a) Conditions: 1 mmol glucose with 100 mg catalyst was set in 12 mL H_2O under 120 °C and 3.0 MPa, H_2 for 5 h; 0.5 mmol cellobiose or sorbitol and 100 mg catalyst was operated in 12 mL H_2O under 180 °C and 5.0 MPa H_2 for 5 h. Metal loadings: 10 wt% Ni, 5 wt% Co.

pected, the physical mixture of catalysts gave lower yield of sorbitol than the result of NiCo/HZSM-5 catalyst, 90% conversion of glucose and 86% yield sorbitol were obtained in the test (entry 4). Hence, the excellent performances would be mainly due to the formation of NiCo alloy in NiCo/HZSM-5 catalyst. The results were also compared to HY and MOR zeolites supported catalysts and shown in entry 5, 6. 89% and 81% yields of sorbitol were observed respectively, indicating that HZSM-5 was the best support for NiCo alloy catalyst. Besides, the transformation of cellobiose into sorbitol was also carried out to investigate the catalytic activity for the cleavage of 1,4-β-glucoside C–O bond. As shown in entry 7, after operating at 180 °C for 5 h, full conversion of cellobiose was gave over NiCo/HZSM-5 catalyst with 86% yield of sorbitol. The catalytic activities for monometallic Co/HZSM-5 and Ni/HZSM-5 catalysts were found less effective than the bimetallic catalyst with 8% and 72% yields of sorbitol, respectively. Besides, NiCo alloy catalysts which were supported by AC, HY and MOR, also showed lower yield of sorbitol than NiCo/ZHSM-5 for the conversion of cellobiose. Meanwhile, it would be found that acidic supports (HZSM-5, HY and MOR) were beneficial to the cleavage of 1,4-β-glucoside C–O bond and the formation of sorbitol product. The stability of product was also studied. 92% of sorbitol was reconverted under reaction conditions, reflecting that sorbitol was stable in this system.

3.3 Effects of temperature

With the optimal NiCo/HZSM-5 catalyst, the influence of reaction temperature for the hydrogenation of glucose was also studied. As shown in Figure 4(a), when this conversion was conducted at 100 °C, 63% conversion of glucose was observed with 60% yield of sorbitol. Raising the temperature to 110 °C, the conversion of substrate increased to 80%, while the yield of sorbitol elevated to 72%. 98% yield of sorbitol was achieved at 120 °C with the full conversion of the substrate. However, when the reaction temperature raised to 180 °C, the yield of sorbitol decreased to 94%. The formation of by-product in the mixture may be the main reason for the decreasing of sorbitol. Due to presence of half hemiacetal group in cellobiose, the reactivity of cellobiose was lower than that of *D*-glucose [29]. As shown in Figure 4(b), only 55% of cellobiose was converted at 120 °C with less than 1% yield of sorbitol. Noteworthily, most of the cellobiose converted to cellobitol with 54% yield, which was the reaction intermediate. Raising the temperature to 140 °C, full conversion of cellobiose was observed with 97% yield of cellobitol and <2% yield of sorbitol. Further elevating the temperature to 160 °C gave 5% yield of glucose, while the yield of intermediate cellobitol decreased to 27%. When the reaction was conducted at 180 °C, the intermediate cellobitol was fully converted to sorbitol with 86% yield.

3.4 Effect of H_2 pressure

Hydrogen pressure played another key role in the synthesis of sorbitol. The effect of hydrogen pressure on conversion of glucose and cellobiose was shown in Figure 5. It can be seen that the conversion of glucose was closely dependent on H_2 pressure. However, the conversion of cellobiose was not obviously affected by H_2 pressure. As shown in Figure 5(a), when the H_2 pressure was 1 MPa, the conversion of glucose reached to 77% with 74% yield of sorbitol. Increasing H_2 pressure to 2 MPa, the yield of sorbitol increased up to 90% accordingly. Further increasing H_2 pressure to 3 MPa,

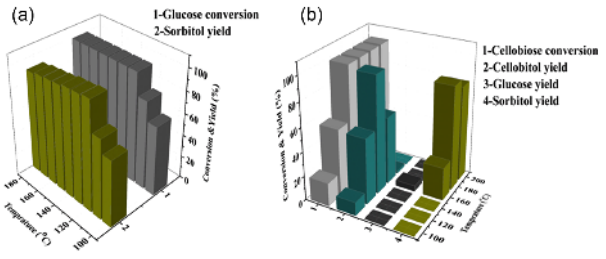

Figure 4 Effect of different temperatures on (a) conversion of *D*-glucose and (b) conversion of cellobiose to *D*-sorbitol. Reaction conditions: (a) 1.0 mmol of *D*-glucose, 100 mg NiCo/HZSM-5, 3.0 MPa H_2 pressure, 5 h, 12 mL H_2O; (b) 0.5 mmol of cellobiose, 100 mg NiCo/HZSM-5, 5.0 MPa H_2 pressure, 5 h,12 mL H_2O (color online).

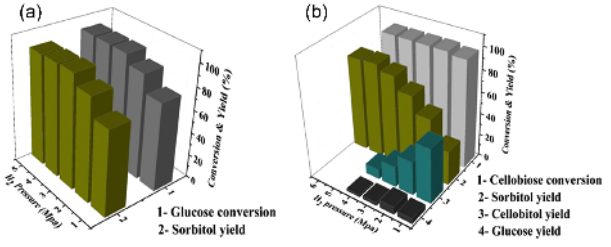

Figure 5 Effect of H_2 pressure on (a) conversion of glucose and (b) conversion of cellobiose to *D*-sorbitol. Reaction conditions: (a) 1.0 mmol of *D*-glucose, 100 mg NiCo/HZSM-5, 120 °C, 5 h, 12 mL H_2O; (b) 0.5 mmol of cellobiose, 100 mg NiCo/HZSM-5, 180 °C, 5 h, 12 mL H_2O (color online).

glucose was fully converted with 98% yield of sorbitol.

When cellobiose was set as the substrate, 98% conversion of cellobiose was obstained under 1 MPa H_2 with 50% yield of cellobitol, 5% yield of glucose and 31% yield of sorbitol, respectively. Increasing H_2 pressure to 2 MPa, the yield of intermediate cellobitol was regularly decreased to 31% with 54% yield of sorbitol and 7% yield of glucose. At 3 MPa H_2 pressure, the yield of cellobitol further decreased to 19% with 69% yield of sorbitol and 3% yield of glucose. A full conversion of cellobitol was conducted under 5 MPa H_2 producing 86% yield of sorbitol. Further elevating the H_2 pressure to 6 MPa did not give a higher yield of sorbitol.

3.5 Kinetic studies and reaction pathway

To investigate the kinetic studies, the effect of reaction time on catalytic conversion of glucose and cellobiose over NiCo/HZSM-5 catalysts was also studied. As shown in Figure 6, the conversion of glucose and the yield of sorbitol were both dependent on reaction time. After 1 h, only 33% conversion of glucose was observed with 30% yield of sorbitol. The conversion of glucose reached to 91% with 88% yield of sorbitol, when the reaction time increased to 4 h. Full conversion of glucose was obtained with 98% yield of sorbitol when the reaction time increased to 5 h.

To investigate the reaction processes of 1,4-β-glucoside C–O bond cleavage, several reactions were done using cellobiose as substrate in the kinetics studies. As shown in Figure 6(b), after 0.5 h operation, 79% yield of cellobitol was obtained with 7% yield of sorbitol. When the reaction time increased to 1 h, cellobiose was completely converted with 57% yield of cellobitol, 6% yield of glucose and 30% yield of sorbitol respectively. The yield of cellobitol decreased to 43% after elevating the reaction time to 2 h, while the 5% yield of glucose was given with 49% yield of sorbitol. After 3 h reaction, the yield of cellobitol decreased to 30%, while the yields of glucose and sorbitol increased to 6% and 63%, respectively. After 4 h operation, only 13% yield of intermediate cellobitol was remained with 5% yield of glucose and 78% yield of sorbitol, respectively. When the reaction time prolonged to 5 h, cellobitol was completely converted with 86% yield of sorbitol.

Based on above results, intermediate cellobitol draw our attentions. Although, several studies have been made on the conversion of cellobiose to sorbitol for monitoring the cleavage of 1,4-β-glycoside bond via tandem hydrolysis and hydrogenation [17,30]. Only few studies discussed the route of reaction via cellobitol intermediate [17]. Wang *et al.* [4] observed that the formation of intermediate cellobitol was followed by the hydrogenation of cellobiose over Ru/CNT

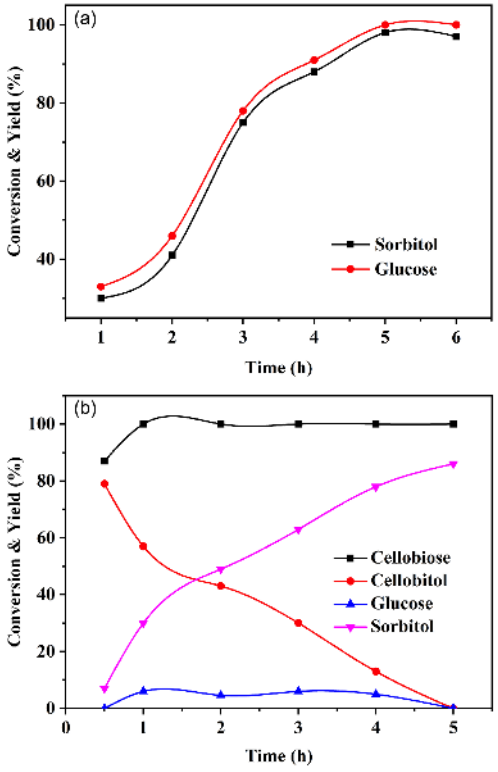

Figure 6 (a) Effects of reaction time on (a) conversion of glucose to sorbitol and (b) conversion of cellobiose to *D*-sorbitol. Reaction conditions: (a) 1.0 mmol of *D*-glucose, 100 mg NiCo/HZSM-5, 120 °C, 3.0 MPa H_2 pressure, 12 mL H_2O; (b) 0.5 mmol of cellobiose, 100 mg NiCo/HZSM-5, 180 °C, 5 MPa H_2 press (color online).

catalyst in aqueous phase. The kinetic studies made by Palkovits *et al.* [17]. further reported the initial hydrogenation cellobiose to give cellobitol followed by hydrolysis to sorbitol as a major pathway over Ru/C in combination with heteropoly acid. Similar findings were also reported by Heeres *et al.* [11] over Ru/CMK-3 catalyst.

Based on experimental results and previous reports, a possible reaction route for the conversion of cellobiose over NiCo/HZSM-5 catalysts was proposed in Scheme 1. At first step, the cellobiose (**1**) was converted to cellobitol (**2**) over bimetallic NiCo/HZSM-5 catalyst via hydrogenation of C–O bond of pyranose ring. Then, the subsequent transformation of cellobitol (**2**) to sorbitol (**4**) was conducted over NiCo/HZSM-5 catalyst via hydrolysis. Meanwhile, glucose (**3**) formed during the 1,4-β-glycoside bond hydrolysis of cellobitol (**2**). At the end, formed glucose (**3**) was converted to sorbitol (**4**) through catalyzed hydrogenation process.

3.6 Stability of NiCo/HZSM-5 catalyst

The catalytic stability is another important parameter in the catalyst estimation. To conduct recycle tests of catalyst, the NiCo/HZSM-5 catalyst was separated and collected after each reaction. As shown in Figure 7, the catalytic conversion of cellobiose was constant in 100% after three recycle operations. However, the yield of sorbitol gradually decreased from 86% to 64%. With the reducing of sorbitol, the yields of glucose and cellobitol got slightly increased. In the first run, no yield of cellobitol intermediate was observed. However, after second and third runs, 13% and 21% yields of cellobitol were present, respectively. Based on above investigations, it would be known that the catalytic hydrogenation activity was mainly due to the metal species, while the acidic sites were responsible for the catalytic hydrolysis. Since full conversions of cellobiose were obtained in each recycle test,

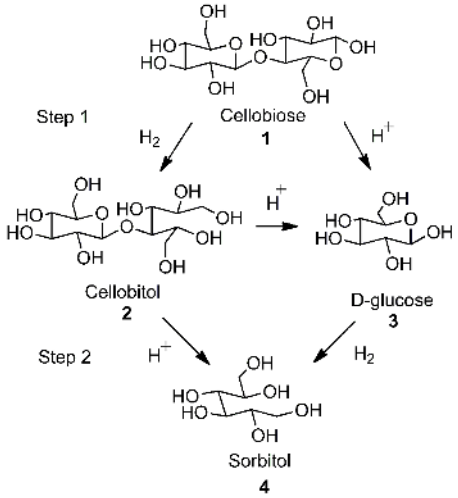

Scheme 1 Reaction route for the conversion of cellobiose with NiCo/HZSM-5.

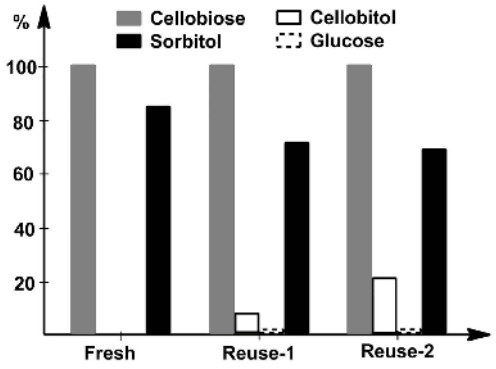

Figure 7 Recycling tests of NiCo/HZSM-5 catalyst for the conversion of cellobiose.

it would be inferred that the catalytic activity of metal species was basically remained during the recycle. However, the reducing of sorbitol and the increasing of cellobitol proved the deactivation of acidic sites, which were the key for the cleavage of 1,4-β-glycoside bond. The deactivation of acidic sites would be due to the polymerization of by-products which formed over the catalyst during the transformation of cellobiose.

4 Conclusions

In summary, an efficient NiCo/HZSM-5 was fabricated through step impregnation, and the synthesis of sorbitol from cellobiose was achieved under mild conditions. 86% yield of sorbitol was observed from full conversion of cellobiose over NiCo/HZSM-5 under 180 °C, 5 MPa H_2 within 5 h, which were hard to realize in non-noble mono-metallic catalysts reports. The excellent performance would be attributed to the formation of NiCo alloy and highly dispersed metal nanoparticles. In the kinetic studies, cellobbitol was detected as an intermediate in the reaction mixture. Meanwhile, a few amount of glucose was observed. It was confirmed that the hydrogenation of cellobiose was faster than the hydrolysis process. Additionally, in the recycle test, NiCo/HZSM-5 catalyst also showed a well catalytic stability. NiCo alloy was relatively stable. The deactivation of catalyst was mainly due to the cover of acidic sites.

Acknowledgements This work was supported by the National Natural Science Foundation of China (21732006, 21572212), the Strategic Priority Research Program of the CAS (XDB20000000, XDA21060101), Ministry of Science and Technology of China (2017YFA0303502), the Fundamental Research Funds for the Central Universities (WK3530000001) and the Major Program of Development Foundation of Hefei Center for Physical Science and Technology (2017FXZY001). The authors thank the Hefei Leaf Co., Ltd. and Anhui Kemi Machinery Technology Co., Ltd. for free samples and equipment that helped us conduct this study.

Conflict of interest The authors declare that they have no conflict of interest.

Supporting information The supporting information is available online at

http://chem.scichina.com and http://link.springer.com/journal/11426. The supporting materials are published as submitted, without typesetting or editing. The responsibility for scientific accuracy and content remains entirely with the authors.

1 Xia Q, Chen Z, Shao Y, Gong X, Wang H, Liu X, Parker SF, Han X, Yang S, Wang Y. *Nat Commun*, 2016, 7: 11162
2 Lazaridis PA, Karakoulia S, Delimitis A, Coman SM, Parvulescu VI, Triantafyllidis KS. *Catal Today*, 2015, 257: 281–290
3 Serrano-Ruiz JC, Luque R, Sepúlveda-Escribano A. *Chem Soc Rev*, 2011, 40: 5266–5281
4 Deng W, Liu M, Tan X, Zhang Q, Wang Y. *J Catal*, 2010, 271: 22–32
5 Zhu W, Yang H, Chen J, Chen C, Guo L, Gan H, Zhao X, Hou Z. *Green Chem*, 2014, 16: 1534–1542
6 Kobayashi H, Ito Y, Komanoya T, Hosaka Y, Dhepe PL, Kasai K, Hara K, Fukuoka A. *Green Chem*, 2011, 13: 326–333
7 Werpy T, Petersen G, Aden A, Bozell J, Holladay J, White J, Manheim A, Eliot D, Lasure L, Jones S. *Top Value Added Chemicals From Biomass. Volume 1-Results of Screening for Potential Candidates From Sugars and Synthesis Gas*. Report No. DOE/GO-102004-1992. Department of Energy Washington DC, 2004
8 Huber GW, Cortright RD, Dumesic JA. *Angew Chem Int Ed*, 2004, 43: 1549–1551
9 Zada B, Chen M, Chen C, Yan L, Xu Q, Li W, Guo Q, Fu Y. *Sci China Chem*, 2017, 60: 853–869
10 Huang YB, Fu Y. *Green Chem*, 2013, 15: 1095–1111
11 Yin W, Tang Z, Venderbosch RH, Zhang Z, Cannilla C, Bonura G, Frusteri F, Heeres HJ. *ACS Catal*, 2016, 6: 4411–4422
12 Yan N, Zhao C, Luo C, Dyson PJ, Liu H, Kou Y. *J Am Chem Soc*, 2006, 128: 8714–8715
13 Yabushita M, Kobayashi H, Fukuoka A. *Appl Catal B-Environ*, 2014, 145: 1–9
14 Almeida JMAR, Da Vià L, Demma Carà P, Carvalho Y, Romano PN, Peña JAO, Smith L, Sousa-Aguiar EF, Lopez-Sanchez JA. *Catal Today*, 2017, 279: 187–193
15 Ribeiro LS, Delgado JJ, Órfão JJM, Pereira MFR. *Appl Catal B-Environ*, 2017, 217: 265–274
16 Romero A, Nieto-Márquez A, Alonso E. *Appl Catal A-Gen*, 2017, 529: 49–59
17 Negahdar L, Oltmanns JU, Palkovits S, Palkovits R. *Appl Catal B-Environ*, 2014, 147: 677–683
18 Chen MY, Chen CB, Zada B, Fu Y. *Green Chem*, 2016, 18: 3858–3866
19 Khodakov AY, Griboval-Constant A, Bechara R, Zholobenko VL. *J Catal*, 2002, 206: 230–241
20 Wang S, Yin Q, Guo J, Ru B, Zhu L. *Fuel*, 2013, 108: 597–603
21 Gao X, Tan Z, Hidajat K, Kawi S. *Catal Today*, 2017, 281: 250–258
22 Chen B, Guo H, Wan Z, Xu X, Zhang H, Zhao D, Chen X, Zhang N. *Energy Fuels*, 2018, 32: 5527–5535
23 Rout L, Kumar A, Dhaka RS, Dash P. *RSC Adv*, 2016, 6: 49923–49940
24 Lee K, Savadogo O, Ishihara A, Mitsushima S, Kamiya N, Ota K. *J Electrochem Soc*, 2006, 153: A20
25 Hu X, Lu G. *J Mol Catal A-Chem*, 2007, 261: 43–48
26 Takanabe K, Nagaoka K, Nariai K, Aika K. *J Catal*, 2005, 232: 268–275
27 Li L, Anjum DH, Zhu H, Saih Y, Laveille PV, D'Souza L, Basset JM. *ChemCatChem*, 2015, 7: 427–433
28 Zhang J, Wang H, Dalai A. *J Catal*, 2007, 249: 300–310
29 Cao Y, Wang J, Kang M, Zhu Y. *RSC Adv*, 2015, 5: 90904–90912
30 Dhepe PL, Fukuoka A. *ChemSusChem*, 2008, 1: 969–975